



The Brazilian Journal of INFECTIOUS DISEASES

www.elsevier.com/locate/bjid



Original article

Development of sandwich-form biosensor to detect *Mycobacterium tuberculosis* complex in clinical sputum specimens



Taha Roodbar Shojaei^a, Mohamad Amran Mohd Salleh^{a,*}, Meisam Tabatabaei^b,
Alireza Ekrami^c, Roya Motallebi^d, Tavoos Rahmani-Cherati^e, Abdollah Hajililou^a,
Raheleh Jorfi^a

^a Institute of Advanced Technology (ITMA), Universiti Putra Malaysia, 43400 Serdang, Selangor, Malaysia

^b Nanosystems Research Team (NRTeam), Microbial Biotechnology and Biosafety Department, Agricultural Biotechnology Research Institute of Iran (ABRII), Karaj, Iran

^c Infectious and Tropical Diseases Research Center, Ahvaz Jundishapur University of Medical Sciences, Ahvaz, Iran

^d Department of Plant Breeding and Biotechnology, College of Agriculture, Shahrekord University, P.O. Box 115, Shahrekord, Iran

^e Research and Development Department, Nanozino, 16536-43181 Tehran, Iran

ARTICLE INFO

Article history:

Received 30 January 2014

Accepted 19 May 2014

Available online 30 August 2014

Keywords:

Mycobacterium tuberculosis complex (MTBC)

Cadmium-telluride quantum dots (CdTe-QDs)

Gold nanoparticles (AuNPs)

Fluorescence resonance energy transfer (FRET)

Sandwich-form FRET-based biosensor

ABSTRACT

Mycobacterium tuberculosis, the causing agent of tuberculosis, comes second only after HIV on the list of infectious agents slaughtering many worldwide. Due to the limitations behind the conventional detection methods, it is therefore critical to develop new sensitive sensing systems capable of quick detection of the infectious agent. In the present study, the surface modified cadmium-telluride quantum dots and gold nanoparticles conjunct with two specific oligonucleotides against early secretory antigenic target 6 were used to develop a sandwich-form fluorescence resonance energy transfer-based biosensor to detect *M. tuberculosis* complex and differentiate *M. tuberculosis* and *M. bovis* Bacille Calmette–Guerin simultaneously. The sensitivity and specificity of the newly developed biosensor were 94.2% and 86.6%, respectively, while the sensitivity and specificity of polymerase chain reaction and nested polymerase chain reaction were considerably lower, 74.2%, 73.3% and 82.8%, 80%, respectively. The detection limits of the sandwich-form fluorescence resonance energy transfer-based biosensor were far lower (10 fg) than those of the polymerase chain reaction and nested polymerase chain reaction (100 fg). Although the cost of the developed nanobiosensor was slightly higher than those of the polymerase chain reaction-based techniques, its unique advantages in terms of turnaround time, higher sensitivity and specificity, as well as a 10-fold lower detection limit would clearly recommend this test as a more appropriate and cost-effective tool for large scale operations.

© 2014 Elsevier Editora Ltda. All rights reserved.

* Corresponding author.

E-mail addresses: asalleh@upm.edu.my, amransalleh@yahoo.co.uk (M.A. Mohd Salleh).

<http://dx.doi.org/10.1016/j.bjid.2014.05.015>

1413-8670/© 2014 Elsevier Editora Ltda. All rights reserved.

Introduction

Tuberculosis (TB) is one of the major chronic infectious diseases caused by *Mycobacterium tuberculosis* (MTB) and represents a global health concern.^{1,2} It is posing a threat even in the developed countries, because it may emerge as an obstacle of human immune deficiency syndrome.² TB is spread in the air and can affect all parts of human body but mostly lungs.³ MTB was reported to have caused 1.4 million deaths and 8.5 million incident cases across the world only in the year 2011.³

Beside MTB, the other members of what is commonly referred to as the *M. tuberculosis* complex including *M. africanum*, *M. microti*, and *M. bovis* may also cause TB infection. The only available vaccine against MTB is the attenuated *M. bovis* strains or Bacille Calmette–Guerin (BCG) which causes some cross-reactivity or false-positive results during the detection process.^{4,4} Therefore, developing an accurate and reliable detection technique capable of differentiating infected samples from those vaccinated is also required.

On the other hand, early detection is so critical to avoid a TB epidemic. To achieve that, many techniques have been developed and widely applied to date such as bacteria's physical, physiological and biochemical characteristics as well as polymerase chain reaction (PCR)-based techniques.^{2,5–11} More recently WHO recommended Xpert MTB/RIF detection technique as a primary sensitive diagnostic test.¹² However, all these techniques have a number of shortcomings and as a result, there is still a growing desire to accomplish a simple, rapid, sensitive and specific detection method to differentiate MTBC-infected samples from vaccinated samples with an affordable cost.^{2,8,11,13,14}

The conserved genomic region of 6-kDa early secretory antigenic target 6 (ESAT-6) has been found of high homology among the different species of mycobacteria and has been used in the most studies to detect MTBC.^{15,16} On the other hand, to differentiate BCG vaccinated samples from MTB-infected samples, the ESAT-6 genomic region which is eliminated in all available BCG strains but present in the MTB complex was utilized.^{15,16} In addition, during the last decade, by applying nano-sized materials in biological detection and biological imaging aspects, the clinical diagnostics field has improved dramatically by developing rapid and sensitive methods at lower cost.^{17,18} Semiconductor nanocrystals, also known as quantum dots (QDs), are one of the most attractive fluorescent nanoparticles which have been widely applied in bio-detection processes.¹⁹ QDs are considered as alternative fluorescent probes for their unique optical properties such as high fluorescence yields, high photo-stability and narrow symmetric emission spectrum.¹⁹ Moreover, the symmetric emission spectra of QDs have nominated them as an appropriate donor molecule for Förster resonance energy transfer (FRET)-based sensors,^{18,20,21} in which the electronic excitation energy of a donor molecule is transferred to a nearby acceptor molecule via a dipole–dipole interaction between the donor/acceptor pair.²² Case in point, the QDs broadly used as bio-sensors by immobilizing with particular probes to detect a specific target nucleotide.²³

Gold nanoparticles (AuNPs) have also been utilized widely in the detection of specific RNA or DNA molecules due to their unique optical properties.^{24,25} AuNPs have remarkably high extinction coefficients and a broad absorption spectrum, allowing higher sensitivity in optical detection techniques than traditional dyes and designating AuNPs as a suitable acceptor for FRET.^{23,26} Due to the fact that, the emission and absorption spectrum of CdTe-QDs and AuNPs significantly overlap in 530 nm, the emission of the QDs is quenched when associated with oppositely charged AuNPs.^{23,27}

In the present study, QDs were immobilized with a specific oligonucleotide (P1) and AuNPs was conjunct with another specific oligonucleotide (P2) against ESAT-6 region to develop a specific and sensitive sandwich-form FRET-based biosensor to detect and differentiate *M. tuberculosis* complex from BCG rapidly, accurately, and economically (Fig. 1). Moreover, the validity of sandwich-form FRET-based biosensor in comparison with culture, PCR and Nested PCR was evaluated.

Materials and methods

Samples

In the present study, 50 clinical samples (all subjects were HIV negative) were collected from sputum specimens of patients who were suspected to have tuberculosis in Tehran province hospitals, Iran (between December of 2005 and November 2008). The used procedures in the present study were in accordance with the ethical standards of the responsible committee on human experimentation from each participating hospital. The patients have given informed prior to participating in the research. The decontamination and cultivation of samples were carried out in the hospitals. Samples were decontaminated by using *N*-acetylcysteine–NaOH procedures. The mentioned samples were earlier analyzed and determined by using a cultivation technique as a gold-standard detection method by incubation 250 μ L of *Mycobacterium* in the Lowenstein–Jensen media at 37 °C in humid atmosphere containing 5% CO₂.²⁸

Primers and probes

In the PCR-based-detection phases, the primer sets were ordered based on an insertion sequence of the IS6110 gene region (Table 1).^{29,30}

In the nano-based detection phase, two different oligonucleotide probes were used based on the conserved genomic regions of ESAT-6¹⁶ to detect MTBC and differentiate between BCG and other *Mycobacterium* species simultaneously (Table 1). The 5' end of the first oligonucleotide probe (P1) was linked to QDs by NH₂ and the 3' end of the second oligonucleotide probe (P2) was linked to AuNPs by SH to facilitate the hybridization process. The probes were purchased from Invitrogen (Shanghai Invitrogen Biotechnology Co).

DNA detection by PCR and nested PCR assays

According to a DNA extraction technique described elsewhere,³¹ the chromosomal DNA was extracted utilizing

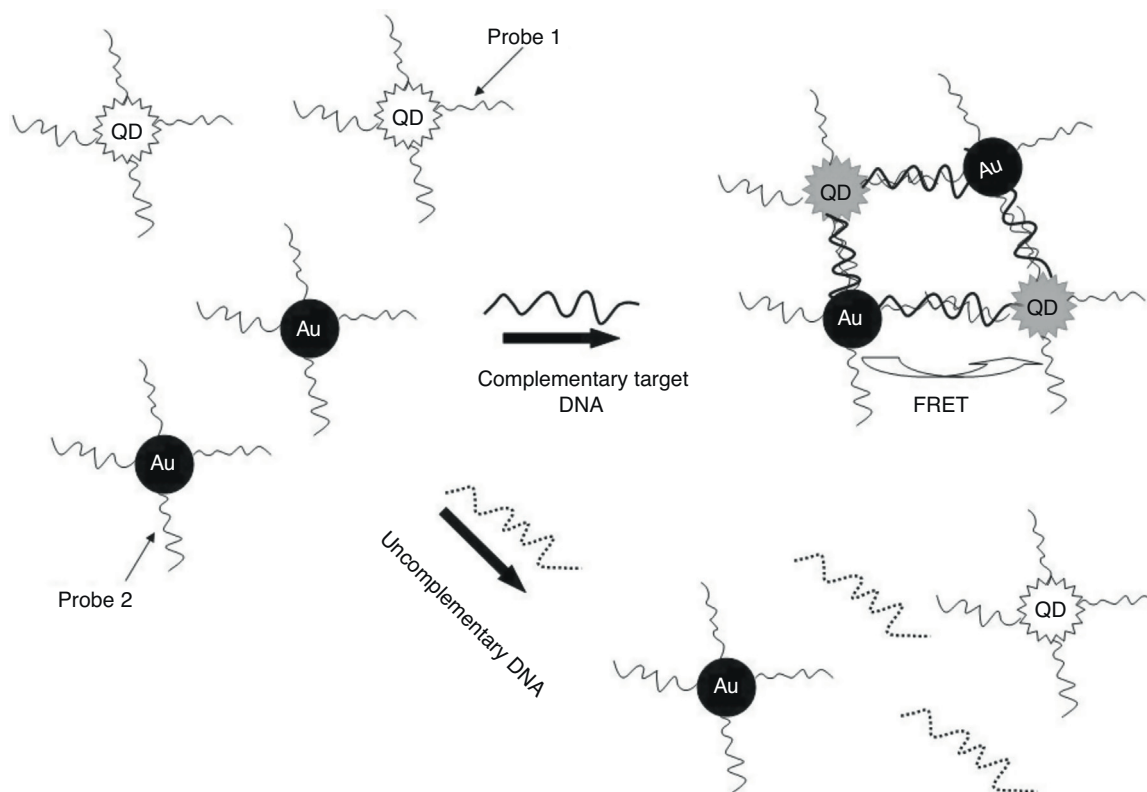


Fig. 1 – Sandwich-form FRET-based biosensor schematic. In the presence of the target the AuNPs/P2 moiety optically quenched the QDs/P1 moiety. Presence of the target molecules turned the AuNPs/P2 into a fluorescence acceptor close enough to the QDs/P1 resulting in a FRET signal.

Table 1 – Characteristics of DNA oligonucleotide primers and probes utilized for detection of MTBC by PCR, nested PCR and nanobiosensor.

| Technique | Sequence (5' → 3') | Genomic region |
|-----------------|---|----------------------------|
| PCR | R: CCTGCGAGCGTAGGCGTCGG F: CTCGTCCAGCGCGCTTCGG | IS6110 |
| Nested PCR | Outer set | IS6110 |
| | Pt8: GTGCGGATGGTCGCAGAGAT Pt9: GTGCGGATGGTCGCAGAGAT | |
| | Inner set | |
| | TB290: GCGGGACAACGCCGAAT-GCGAA Pt9: GTGCGGATGGTCGCAGAGAT | |
| Pre-preparation | R: ACGAAGCTTTGCGAACATCCCAGT-GACGTT F: AATCGGATCCATGACA-GAGCAGCAGTGGAAATTC | ESAT-6 ESAT-6 |
| | R: ACGAAGCTTTGCGAACATCCCAGT-GACGTT F: AATCGGATCCATGACA-GAGCAGCAGTGGAAATTC | ESAT-6 ESAT-6 ESAT-6 |
| Nanobiosensor | P1: NH ₂ (CH ₂) ₆ -GTAAGTAAGGGAGGAAC P2: TGCTCCCTTCGTCAGG-(CH ₂) ₆ -SH | |

proteinase K and phenol:chloroform, and was subsequently precipitated by using isopropanol and ethanol. To detect MTBC DNA, the PCR and nested PCR assays were performed by utilizing BioRad thermocycler (BioRad, CA, USA) based on the protocols described by Eisenach et al.³² and Wilson et al.³³ To examine the existence and size of the amplified fragments, 2% agarose gel and the Gene Ruler™ 50bp DNA Ladder (Fermentas) were used. Visualization of agarose gel was done by ethidium bromide and gels were photographed with UVP Bio Doc-It™ system CCD camera (UVP Inc., Upland, USA). Moreover, to determine the detection limits of the used methods, different dilutions of a known chromosomal DNA stock were used.

Synthesis of AuNPs

The AuNPs were synthesized through the citrate reduction method by adding trisodium citrate solution to 170 mgL⁻¹ HAuCl₄ under stirring and temperature condition. After a color shift in solution from yellow to red, the stirring and heating were stopped and the solution was stored at 4 °C.²⁴ Afterwards, the synthesized AuNPs were characterized by transmission electron microscope (TEM) (Hitachi H-7100) and particles diameter size were determined using UTHSCSA Image Tool (University of Texas).

Synthesis of CdTe QDs

The NaHTe solution was prepared by adding 2 mM of NaBH₄ and tellurium powder in 50 mL of distilled water. To prepare CdTe QDs, 10 mM of CdCl₂ and 25 mM of TGA were dissolved in 250 mL distilled water under stirring and the pH was adjusted to 11 by using NaOH solution. Subsequently, the NaHTe solution was added to the solution under N₂ protection under stirring for 25 min. Finally, this mixture was heated to boil at 100 °C for 2 h.³⁴ Then, the synthesized AuNPs were characterized by TEM (Hitachi H-7100) and particles diameter size were determined using UTHSCSA Image Tool (University of Texas).

Conjugation of the first oligonucleotide (P1) on the CdTe QDs surface

Conjugation of the first probe on the surface of CdTe QDs was carried out by mixing 1 mL of CdTe QDs, 20 µg of the P1 and 50 µL of 1-ethyl-3-(dimethylaminopropyl) carbodiimide hydrochloride (EDC). The solution was mixed in 50 mM dipotassium phosphate buffer solution (pH = 6) at room temperature.²³

Assembling of the second oligonucleotide (P2) on the AuNPs surface

To prepare the self-assembly of the probes onto the AuNPs surface, 10 mL of AuNPs solution and 20 µg of the P2 were mixed at room temperature for about 10 h. Afterwards, the solution was added into a dipotassium phosphate buffer solution (pH = 6.0). To purify the AuNPs-probe, centrifugation was performed at 18,000 rcf for 25 min and the pellet was resuspended in dipotassium phosphate buffer solution.²³

Pre-preparation of clinical sputum specimens for biosensor procedure

The clinical sputum samples were first used for PCR amplification of ESAT-6 gene (Table 1).

The PCR was performed by utilizing BioRad thermocycler (BioRad, CA, USA) based on the protocols described by Eisenach et al.³² Subsequently, PCR products were analyzed by sandwich-form FRET-based biosensor.

Sandwich-form FRET-based biosensor

To perform the sandwich-form FRET-based biosensor assay, 10 µL of QDs/P1 solution, 10 µL of AuNPs/P2 solution and 10 µL of PCR product were mixed in a tube. Subsequently, denaturation and annealing of samples with the immobilized oligonucleotides were carried out at 94 °C for two min and at 65–68 °C for two min, respectively, using a BioRad thermocycler (BioRad, CA, USA). Then, the fluorescence intention spectra were recorded by using a spectrophotometer. Baseline changes estimated by subtracting the second run from the first run and the threshold for negative sample was estimated at 8.2 ± 3.

Fluorescence procedure

The fluorescence spectra were monitored by using a PD-3000UV ultraviolet-visible spectrophotometer (Appel, Japan). The excitation wavelength (excitation wavelength of QDs) was set at 370 nm and the emission spectra were probed between 400 and 680 nm as the AuNP's (quencher) emission was located in the range of 570–650 nm. The excitation and emission bandwidth of 5 nm was used.

Data analysis

Data analysis was performed using the SAS 6.12 (SAS Institute, Cary, NC), and diagnostic sensitivity and specificity were determined using usual formula.

$$\text{Sensitivity} = \frac{\text{True Positive}}{\text{True Positive} + \text{False Negative}} \times 100$$

$$\text{Specificity} = \frac{\text{True Negative}}{\text{False Positive} + \text{True Negative}} \times 100$$

The other statistical parameters were calculated using an online clinical calculator available at <http://www.vassarstats.net/clin1.html>.

Results

As mentioned earlier, cultivation technique was considered the gold-standard detection method in order to compare the other techniques used, i.e. PCR, nested PCR and the sandwich-form FRET-based biosensor. In presence of *M. tuberculosis* infection in the sample, PCR and nested PCR products of about 123 bp and 360 bp were observed using IS6110 primer sets (Fig. 2), and 60% (30/50) and 64% (32/50) of the specimens were found positive, respectively. On the other hand, out of the 50 samples tested by the sandwich-form FRET-based biosensor, 70% (35/50) were found positive. Interestingly, out of those 35 positive samples by the FRET-based biosensor, only 33 (94.2%) were culture-positive. Thus, two positive samples by FRET-based biosensor assay were reported negative by the culture-based method. Furthermore, out of the 35 positive samples, only 27 (77.1%) and 30 (85.7%) were detected by PCR and nested PCR techniques, respectively.

Therefore, the overall sensitivity and specificity of the PCR method in relation to the cultivation method for detection of MTBC was 74.2% (95% CI 56.4–86.8) and 73.3% (95% CI 44.8–91.0), respectively (Table 2). Besides, sensitivity and specificity of the nested PCR method in relation to the cultivation technique were 82.8% (95% CI 65.7–92.8) and 80% (95% CI 51.3–94.6), respectively (Table 2). The samples were first utilized for PCR amplification of ESAT-6 gene and subsequently PCR products were analyzed by sandwich-form FRET-based biosensor. The results obtained revealed that the sandwich-form FRET-based biosensor versus cultivation demonstrated in detecting *Mycobacterium* had sensitivity and specificity of 94.2% (95% CI 79.4–99.0) and 86.6% (95% CI 58.3–97.6), respectively (Table 2).

To determine the characteristics of the donors and acceptors in the sandwich-form FRET-based biosensor, the QDs and AuNPs were characterized by using TEM. The TEM image

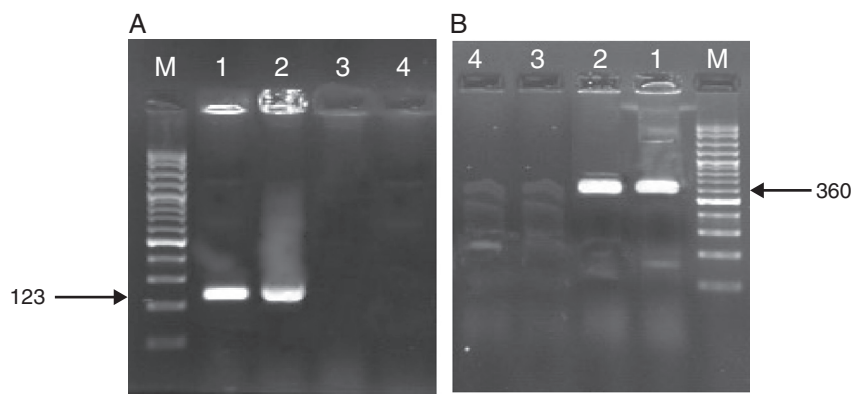


Fig. 2 – Amplified products of MTBC by PCR and nested PCR methods. (A) PCR products M: Gene Ruler™ 50bp DNA Ladder, 1: positive control sample, 2: clinical positive sample, 3: negative control sample, 4: clinical negative sample. (B) Nested PCR products (second round) M: Gene Ruler™ 50bp DNA Ladder, 1: clinical positive sample, 2: positive control sample, 3: negative control sample, 4: clinical negative sample.

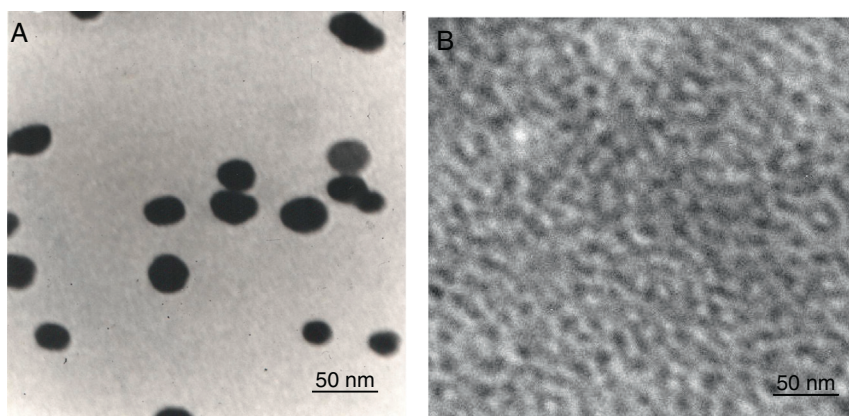


Fig. 3 – TEM image of synthesized AuNPs (A) and CdTe-QDs (B).

showed that the QD and Au nanoparticles have a spherical morphology and suitable monodispersity (Fig. 3A and B). The QDs and AuNPs particle size were determined at 6 nm and 8 nm, respectively. From the mechanistic point of view, in the

solution containing only the QDs/P1 and AuNPs/P2 (negative control), the fluorescence spectrum was recorded at 50 AU, while in presence of *Mycobacterium* DNA (target molecule), a significant downward shift in the spectrum peaking at 10 AU

Table 2 – Comparison between FRET-based biosensor, PCR and nested PCR versus culture method for detection of *Mycobacterium tuberculosis* in 50 sputum clinical samples.

| Methods | Cultivation assay | | Value | |
|---------------------------------|-------------------|--------------|---------------|---------------|
| | Positive (n) | Negative (n) | Sensitivity % | Specificity % |
| <i>FRET-based nanobiosensor</i> | | | | |
| Positive | 33 | 2 | 94.2 | 86.6 |
| Negative | 2 | 13 | | |
| Total | 35 | 15 | | |
| <i>PCR</i> | | | | |
| Positive | 26 | 4 | 74.2 | 73.3 |
| Negative | 9 | 11 | | |
| Total | 35 | 15 | | |
| <i>Nested PCR</i> | | | | |
| Positive | 29 | 3 | 82.8 | 80.0 |
| Negative | 6 | 12 | | |
| Total | 35 | 15 | | |

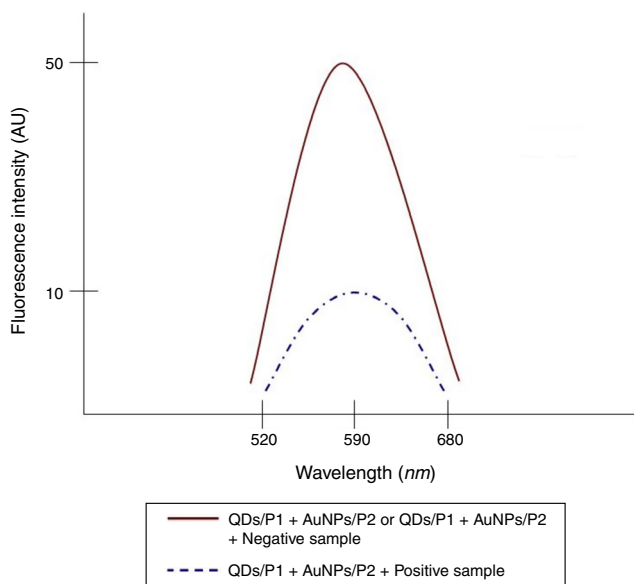


Fig. 4 – Fluorometric peaks of QDs/P1 + AuNPs/P2 solution and solution contained QDs/P1 + AuNPs/P2 + positive sample obtained by spectrophotometer.

was observed (Fig. 4). The emission spectrum of the QDs and absorption spectrum of AuNPs demonstrated maximum overlap that is critical to obtain FRET phenomena (Fig. 5). The FRET efficiency (E) of the presented system was dependent on molar ratio of AuNPs/P2 to QDs/P1. Increases in the molar ratio of AuNPs/P2 to QDs/P1 leads to an increase in the FRET efficiency and the highest FRET efficiency for developed system was achieved at AuNPs/P2 to QDs/P1 molar ratio of 1:10 (Fig. 6)

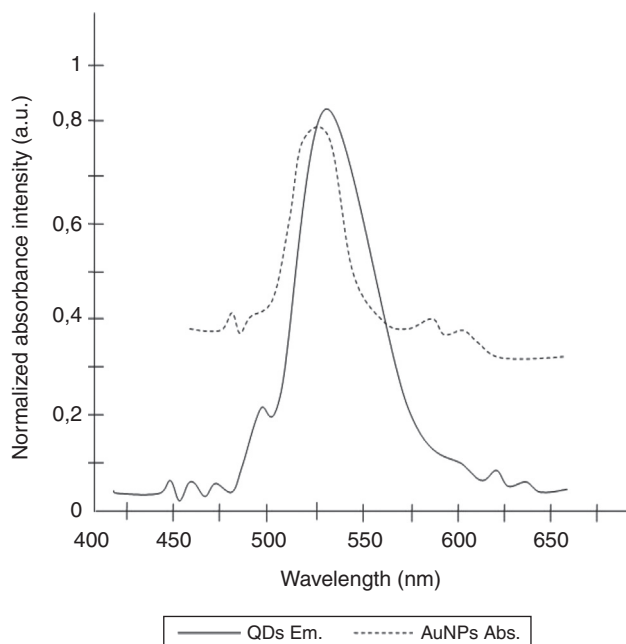


Fig. 5 – Overlap between QDs emission spectrum and AuNPs absorption spectrum.

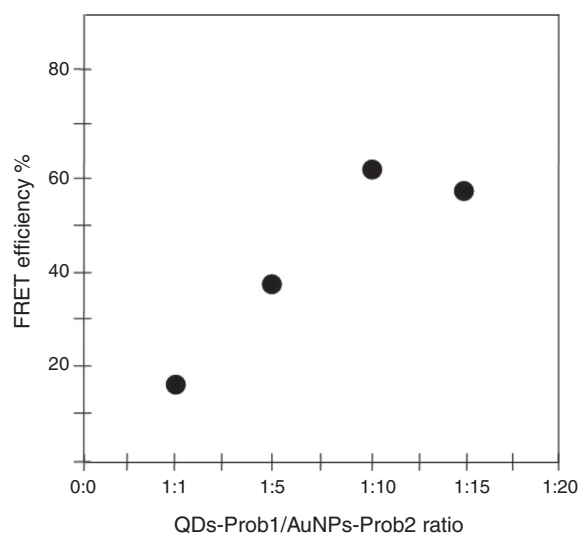


Fig. 6 – Energy transfer efficiency from donor (QDs) to an acceptor (AuNPs) in different molar ratio of AuNPs/P2 to QDs/P1.

Table 3 – Comparison between PCR, RT-PCR and nanobiosensor detection limits. Presence and absence of specific band in agarose gel in PCR and RT-PCR detection methods were signed positive (+) and negative (-) respectively. In the nanobiosensor technique, observation of downward shift in the fluorometer curve was signed as positive (presence of target) and no shift in the fluorometer curve was signed as negative (absence of target).

| Sample | Volume (fg mL ⁻¹) | PCR | RT-PCR | Nanobiosensor |
|------------------|-------------------------------|-----|--------|---------------|
| Positive control | 200 | + | + | + |
| | 150 | + | + | + |
| | 100 | + | + | + |
| | 50 | - | - | + |
| | 30 | - | - | + |
| | 20 | - | - | + |
| | 10 | - | - | + |
| | 5 | - | - | - |
| Negative control | 0 | - | - | - |

Finally, the detection limit of the PCR and nested PCR methods was measured at 100 fg while for the sandwich-form FRET-based biosensor it was 10-fold lower at 10 fg (Table 3).

Discussion

In the oligonucleotide-based detection systems, the important matter concerned is probes specificity against closely related species, and in the case of MTBC detection, the differentiation between BCG vaccinated samples and infected samples. Therefore, utilizing oligonucleotide probes based on conserved region of MTBC, which is deleted in the *M. bovis* BCG, is important. This point was taken into careful consideration in the present study. Therefore, the conserved genomic regions of ESAT-6 was used as the probe to detect MTBC and

differentiate *M. bovis* BCG from other *Mycobacterium* species, due to the high existing homology in the ESAT-6 regions of different *Mycobacterium* species and the absence of this region in BCG strains.

Although, recently WHO recommended Xpert MTB/RIF as a sensitive detection method, it is not available in all countries. Moreover, the widely used methods in the case of clinical TB detection in the region in which the study was conducted are cultivation test and nested PCR; therefore, in this region the newly developed techniques mostly compared with these methods. Due to the insufficient sensitivity and specificity of the PCR-based assays, developing a more sensitive method for the detection of MTBC has been constantly sought. Although, there are different values reported in the published literature, the sensitivity and specificity of PCR assays used for detection of *Mycobacterium* in the present study were in agreement with the findings of Chawla et al.³⁵ and Ekrami et al.²⁸ In the used clinical samples, four cases were found positive by culture but negative by PCR and nested-PCR, which could be considered as false negative results. These observed false results were attributed to the concentration of target molecules in the clinical samples and to the specificity of utilized primers.

In the case of the nested PCR assay, the sensitivity of 82.8% showed that this technique could not be regarded as an ideal technique to detect MTBC, despite of its specificity to be approximately equal to that of the sandwich-form FRET-based biosensor. The lowest detection limit of *Mycobacterium* DNA achieved by using PCR and nested PCR techniques was 100 fg, which was in agreement with earlier reports.^{36,37} This value was remarkably higher than that achieved by using the sandwich-form FRET-based biosensor (10 fg).

In the sandwich-form FRET-based biosensor, the NH₂ linked oligonucleotide (P1) was capable of covalently attaching onto the surface-modified QDs with EDC due to the adsorption tendency of the carboxyl group of EDC and the NH₂ linked to the P1.³⁸ This conjugate showed maximum fluorescence radiation at 548 nm. Second oligonucleotide (P2) could easily self-assemble on AuNPs due to the attraction of SH linked to the P2 and surface of AuNPs.³⁹ Two samples that were positive by culture and negative by nanosensor showed autofluorescent signals during examination. This problem has been previously reported by Ekrami et al.²⁸ Probably, there is a specific problem when clinical samples are tested. Generally, observed interface by autofluorescence can be attributed to natural factors induced by some reagents in clinical samples.²⁸

The TEM image confirmed that the synthesized QD and Au nanoparticles were appropriate for the nanobiosensor designed (Fig. 3). The emission and absorption spectra of CdTe-QDs and AuNPs significantly overlap at 530 nm; therefore, CdTe-QDs and AuNPs could be used successfully as a suitable donor and acceptor pair (Fig. 5). To find out the optimum FRET signal and maximum FRET efficiency, different molar ratios of AuNPs/P2 to QDs/P1 were investigated. Optimum molar ratio of AuNPs/P2 to QDs/P1 was achieved at 1:10 in which FRET efficiency was about 60% (Fig. 6). At higher molar ratios, many oligonucleotide probes immobilized in the surface of AuNPs would remain unhybridized and the FRET efficiency decreased enormously. While, at the lower molar

ratio, decrease in the amounts of AuNPs leads to insufficient energy transfer from QDs near AuNPs molecules and subsequently caused a reduction in the FRET signal (Fig. 6). More specifically, the fluorescence spectrum was 50 AU for the solution containing QDs/P1 and AuNPs/P2, but in the presence of the target a downward shift to 10 AU in the emission spectrum was recorded (Fig. 4). The observed decrease in the fluorescence intensity in the solution containing the targets indicated that FRET process occurred in the QDs/P1-target-AuNPs/P2 complex system. In fact, the AuNPs/P2 moiety in the presence of the target, optically quenched the QDs/P1 moiety, based on the Forster dipole-dipole interaction form.^{27,40} In other words, presence of the target molecules turned the AuNPs/P2 into a fluorescence acceptor close enough to the QDs/P1 resulting in a fivefold FRET signal (Fig. 1). This principle led to a downward shift of the fluorometer curve in comparison with the curve originally obtained for the solution without any target DNA.

To the best of our knowledge, there has been no published reports on combining QDs and AuNPs to detect bacterial targets, although some researchers have developed techniques by using QDs and AuNPs separately.⁴¹⁻⁴³ For instance, Soo et al.⁴² introduced an AuNPs cross-linking approach to detect MTBC. More specifically, the AuNPs were functionalized with thiol modified specific probes. In the presence of target DNA, AuNPs hybridized to the target resulting in aggregation and decrease in absorbance of the solution. The absorbance decreases were accompanied by a shift in solution color from red to reddish purple. On the other hand, in the absence of target DNA, the color and absorbance of the solution were not altered. This assay demonstrated the detection limit of as low as 0.5 pmol of target.⁴²

In another study, Gazouli et al.⁴³ developed a new technique combining QDs with magnetic beads (MBs) to detect *M. tuberculosis* and *M. avium* subsp. *Paratuberculosis* by using DNA extracted from bronchoalveolar lavage specimens. In this technique, two biotinylated oligonucleotide probes were immobilized on the QDs and MBs surface to form a sandwich like hybridization system. In the absence of target, no fluorescence signal was monitored while in the presence of target DNA, red fluorescence color was observed. The detection limit achieved in this assay was reported at 12.5 ng.⁴³

The developed sandwich-form FRET-based biosensor requires small amount of sample; therefore, it could be an appropriate detection technique where limited volumes of samples are available. Moreover, the newly developed biosensor in comparison with the cultivation method showed high sensitivity and specificity. In addition, the developed FRET-based biosensor presented a detection limit of 10 fg which was remarkably lower than the 100 fg of PCR and nested PCR. The cost of sandwich-form FRET-based biosensor developed in the present study was estimated to be slightly more than the PCR-based techniques; but due to the speed and accuracy of the FRET-based nanobiosensor, its large-scale application would be more cost-effective.

Conflicts of interest

The authors declare no conflicts of interest.

REFERENCES

- Shin AR, Shin SJ, Lee KS, et al. Improved sensitivity of diagnosis of tuberculosis in patients in Korea via a cocktail enzyme linked immunosorbent assay containing the abundantly expressed antigens of the K strain of *Mycobacterium tuberculosis*. *Clin Vaccine Immunol*. 2008;15:1788–95.
- Yeo WH, Liu S, Chung JH, Liu Y, Lee KH. Rapid detection of *Mycobacterium tuberculosis* cells by using microtip-based immunoassay. *Anal Bioanal Chem*. 2009;393:1593–600.
- World Health Organization. WHO Global tuberculosis report 2012. Available at: www.who.int/iris/bitstream/10665/75938/1/9789241564502_eng.pdf [accessed June 2012].
- Andersen P, Doherty TM. The success and failure of BCG: implications for a novel tuberculosis vaccine. *Nat Rev Microbiol*. 2005;3:656–62.
- Gill P, Ghalami M, Ghaemi A, Mosavari N, Abdul-Tehrani H, Sadeghizadeh M. Nanodiagnostic method for colorimetric detection of *Mycobacterium tuberculosis* 16S rRNA. *Nanobiotechnology*. 2008;4:28–35.
- Currie CSM, Floyd K, Williams BG, Dye C. Cost, affordability and cost-effectiveness of strategies to control tuberculosis in countries with high HIV prevalence. *BMC Public Health*. 2005;5:130–43.
- Bardarov S Jr, Dou H, Eisenach K, Banaiee N, Ya S, Chan J. Detection and drug-susceptibility testing of *M. tuberculosis* from sputum samples using luciferase reporter phage: comparison with the Mycobacteria Growth Indicator Tube (MGIT) system. *Diag Microbiol Infect Dis*. 2003;45:53–61.
- Hsieh SC, Chang CC, Lu CC, et al. Rapid identification of *Mycobacterium tuberculosis* infection by a new array format-based surface plasmon resonance method. *Nanoscale Res Lett*. 2012;7:180.
- Li H, Turhan V, Chokhani L, Stratton CW, Dunbar SA, Tang YW. Identification and differentiation of clinically relevant mycobacterium species directly from acid-fast bacillus-positive culture broth. *J Clin Microbiol*. 2009;47:3814–20.
- Mdivani N, Li H, Akhalaia M, et al. Monitoring therapeutic efficacy by real-time detection of *Mycobacterium tuberculosis* mRNA in sputum. *Clin Chem*. 2009;55:1694–700.
- Chan ED, Heifets L, Iseman MD. Immunologic diagnosis of tuberculosis: a review. *Tuber Lung Dis*. 2000;80:131–40.
- Vassall A, van Kampen S, Sohn H, et al. Rapid diagnosis of tuberculosis with the Xpert MTB/RIF assay in high burden countries: a cost-effectiveness analysis. *PLoS Med*. 2011;8:e1001120, <http://dx.doi.org/10.1371/journal.pmed.1001120>.
- Van Deun A, Portaels F. Limitations and requirements for quality control of sputum smear microscopy for acid-fast bacilli. *Int J Tuberc Lung Dis*. 1998;2:756–65.
- Chan ED, Reves R, Belisle JT, Brennan PJ, Hahn WE. Diagnosis of tuberculosis by a visually detectable immunoassay for lipoarabinomannan. *Am J Respir Crit Care Med*. 2000;161:1713–9.
- Van Pinxteren LAH, Ravn P, Agger EM, Pollock J, Andersen P. Diagnosis of tuberculosis based on the two specific antigens ESAT-6 and CFP10. *Clin Diagn Lab Immunol*. 2000;7:155.
- Hanif SNM, Al-Attayah R, Mustafa AS. The natural expression of genes encoding major antigens of Rd1 and Rd9 in *M. tuberculosis* and other Mycobacteria. *Mycobact Dis*. 2011;1:2.
- Shi X, Hong T, Walter KL, et al. ING2 PHD domain links histone H3 lysine 4 methylation to active gene repression. *Nature*. 2006;442:96–9.
- Algar WR, Krull UJ. Quantum dots as donors in fluorescence resonance energy transfer for the bioanalysis of nucleic acids, proteins, and other biological molecules. *Anal Bioanal Chem*. 2007;391:1609–18.
- Frasco MF, Chaniotakis N. Semiconductor quantum dots in chemical sensors and biosensors. *Sensors*. 2009;9:7266–86.
- Algar WR, Tavares AJ, Krull U. Beyond labels: a review of the application of quantum dots as integrated components of assays, bioprobes, and biosensors utilizing optical transduction. *Anal Chim Acta*. 2010;673:1–25.
- Zekavati R, Safi S, Hashemi SJ, et al. Highly sensitive FRET-based fluorescence immunoassay for aflatoxin B1 using cadmium telluride quantum dots. *Microchim Acta*. 2013, <http://dx.doi.org/10.1007/s00604-013-1047-y>.
- Wu P, Brand L. Resonance energy transfer: methods and applications. *Anal Biochem*. 1994;218:1–13.
- Dai Z, Zhang J, Dong Q, et al. Adaption of Au nanoparticles and CdTe quantum dots in DNA detection. *Chin J Chem Eng*. 2007;15:791–4.
- Kamelipour N, Mohsenifar A, Tabatabaei M, et al. Fluorometric determination of paraoxon in human serum using a gold nanoparticle-immobilized organophosphorus hydrolase and coumarin 1 as a competitive inhibitor. *Microchim Acta*. 2014;181:239–48.
- Liz-Marzan LM. Tailoring surface plasmons through the morphology and assembly of metal nanoparticles. *Langmuir*. 2006;22:32–41.
- Baptista P, Pereira E, Eaton P, et al. Gold nanoparticles for the development of clinical diagnosis methods. *Anal Bioanal Chem*. 2008;391:943–50.
- Wargnier R, Baranov AW, Maslow VG. Energy transfer in aqueous solutions of oppositely charged CdSe/ZnS core/shell quantum dots and in quantum dot-nanogold assemblies. *Nano Lett*. 2004;4:451–7.
- Ekrani AR, Samarbafe-Zadeh AR, Khosravi A, et al. Validity of bioconjugated silica nanoparticles in comparison with direct smear, culture, and polymerase chain reaction for detection of *Mycobacterium tuberculosis* in sputum specimens. *Int J Nanomed*. 2011;6:2729–35.
- Caviedes L, Lee TS, Gilman RH, et al. Rapid, efficient detection and drug susceptibility testing of *Mycobacterium tuberculosis* in sputum by microscopic observation of broth cultures. *J Clin Microbiol*. 2000;38:1203–8.
- Maurya AK, Kant S, Nag VL, Kushwaha R, Dhole TN. Detection of 123 bp fragment of insertion element IS6110 *Mycobacterium tuberculosis* for diagnosis of extrapulmonary tuberculosis. *Indian J Med Microbiol*. 2012;30:182–6.
- Amita J, Vandana T, Guleria RS, Verma RK. Quality evaluation of mycobacterial DNA extraction protocols for polymerase chain reaction. *Mol Biol Today*. 2002;3:43–50.
- Eisenach KD, Cave MD, Bates JH, Crawford JT. Polymerase chain reaction amplification of a repetitive DNA sequence specific for *Mycobacterium tuberculosis*. *J Infect Dis*. 1990;161:977–81.
- Wilson SM, McNERNEY R, Nye PM, Godfrey-Faussett PD, Stoker NG, Voller A. Progress toward a simplified polymerase chain reaction and its application to diagnosis of tuberculosis. *J Clin Microbiol*. 1993;3:776–82.
- Safarpour H, Safarnejad MR, Tabatabaei M, et al. Development of a quantum dots FRET-based biosensor for efficient detection of *Polymyxa betae*. *Can J Plant Pathol*. 2012;34, <http://dx.doi.org/10.1080/07060661.2012.709885>.
- Chawla K, Gupta S, Mukhopadhyay C, Rao PS, Bhat SS. PCR for *M. tuberculosis* in tissue samples. *J Infect Dev Ctries*. 2009;3:83–7.
- Gengvinij N, Pattanakitsakul S, Chierakul N, Chaiprasert A. Detection of *Mycobacterium tuberculosis* from sputum specimens using one-tube nested PCR. *Southeast Asian J Trop Med Public Health*. 2001;32:114–25.

37. Pao CC, Yen TSB, You JB, Maa JS, Fiss EH, Chang AH. Detection and identification of *Mycobacterium tuberculosis* by DNA amplification. *J Clin Microbiol.* 1990;28:1877-80.
38. Gueroui Z, Libchaber A. Single-molecule measurements of gold-quenched quantum dots. *Phys Rev Lett.* 2004;93:16108-11.
39. Maxwell DJ, Taylor JR, Nie S. Self-assembled nanoparticle probes for recognition and detection of biomolecules. *J Am Chem Soc.* 2002;124:9606-12.
40. Oh E, Hong MY, Lee D, Nam SH, Yoon HC, Kim HS. Inhibition assay of biomolecules based on fluorescence resonance energy transfer (FRET) between quantum dots and gold nanoparticles. *J Am Chem Soc.* 2005;127:3270-1.
41. Liandris E, Gazouli M, Andreadou M, et al. Direct detection of unamplified DNA from pathogenic mycobacteria using DNA-derivatized gold nanoparticles. *J Microbiol Methods.* 2009;78:260-4.
42. Soo PC, Horng YT, Chang KC, et al. A simple gold nanoparticle probes assay for identification of *Mycobacterium tuberculosis* and *Mycobacterium tuberculosis* complex from clinical specimens. *Mol Cell Probes.* 2009;23:240-6.
43. Gazouli M, Liandris E, Andreadou M, et al. Specific detection of unamplified Mycobacterial DNA by use of fluorescent semiconductor quantum dots and magnetic beads. *J Clin Microbiol.* 2010;48:2830-5.